Special issue: Clinical neuroanatomy

Sensitivity to biomechanical limitations during postural decision-making depends on the integrity of posterior superior parietal cortex

Daniel K. Wood [a,b,*,1], *Philippe A. Chouinard* [a,c,1], *Alex J. Major* [a,d] *and Melvyn A. Goodale* [a]

[a] *Department of Psychology and the Brain and Mind Institute, The University of Western Ontario, London, ON, Canada*
[b] *Department of Neurobiology, Northwestern University, Evanston, IL, USA*
[c] *School of Psychology and Public Health, La Trobe University, Bendigo Campus, Bendigo, VIC, Australia*
[d] *Graduate Program in Neuroscience, The University of Western Ontario, London, ON, Canada*

ARTICLE INFO

ABSTRACT

Most object-directed limb movements can be carried out with a comfortable grasp posture. However, the orientation of an object relative to our bodies can sometimes lead us to select an uncomfortable or awkward grasp posture due to limitations imposed by the biomechanics of the arm. In a series of experiments, we identified a network of cortical areas that are engaged during the selection of movement strategies. Neurologically intact participants and two brain-damaged patients with overlapping lesions in the right posterior superior parietal lobule (pSPL) performed a grasp posture selection task in which biomechanical constraints were the primary consideration for selecting an action. The task induced states of bistable actions whereby the same stimulus gave rise to categorically different grasp postures. In a behavioral experiment, the two patients displayed a large range of manual bistability with the contralesional hand, resulting in a higher incidence of awkward grasping postures. In neurologically intact participants, a separate functional magnetic resonance imaging (fMRI) experiment revealed activation of a parieto-frontal network, which included the posterior intraparietal sulcus (pIPS) along the banks of the pSPL that was parametrically modulated by the degree of bistability in grasp posture selection. Superimposing this activation over the patients' structural MRIs revealed that the pIPS/pSPL activation in the neurologically intact participants overlapped with lesioned cortical tissue in both patients; all other areas of activation overlapped with intact cortical tissue in the patients. These results provide converging evidence that the posterior parietal cortex plays a critical role in selecting biomechanically appropriate postures during reach-to-grasp behaviors.

© 2016 Elsevier Ltd. All rights reserved.

* *Corresponding author.* Department of Neurobiology, Northwestern University, Evanston, IL 60208, USA.
   E-mail address: danielkentwood@gmail.com (D.K. Wood).
   [1] The first two authors contributed equally.

1. Introduction

A fundamental question in neuroscience is how animals use sensory information about the environment to guide their movements. Animals must develop knowledge of both environmental dynamics and the limitations and capabilities of their own bodies within the environment. A monkey swinging from branch to branch must know the length and flexibility of its arms, and must rapidly link this knowledge to incoming visual information. A misjudgment could be fatal. Similarly, when something is within reach, misjudgments about biomechanical constraints of the limb can lead to the selection of awkward, inefficient grasp postures. A number of studies have explored how human and non-human primates use visual information to select movements on the basis of the anticipated biomechanical costs of alternative movement strategies (Cos, Bélanger, & Cisek, 2011; Cos, Medleg, & Cisek, 2012; Rosenbaum et al., 1990; Sabes & Jordan, 1997; Zander, Weiss, & Judge, 2013). Yet, the neural circuits that mediate this behavior have not been identified.

The cortical visual system is divided into two separate streams: a ventral stream for perceptual analysis and a dorsal stream for the control of visually guided movement (Goodale & Milner, 1992; Goodale et al., 1994). Both streams process object orientation and shape, and both streams appear to process aspects of body morphology that would be relevant to postural decision-making. For example, structures in the ventral stream play a critical role in the processing of the morphology of bodies, both of others (Urgesi, Calvo-Merino, Haggard, & Aglioti, 2007; Urgesi, Candidi, Ionta, & Aglioti, 2007) and of the self during executed or imagined limb movement (Astafiev, Stanley, Shulman, & Corbetta, 2004; Ferri, Frassinetti, Ardizzi, Costantini, & Gallese, 2012). Meanwhile, parietal circuits in the dorsal stream are involved in building and maintaining a representation of body morphology and mechanics (Bonda, Frey, & Petrides, 1996; Bonda, Petrides, Frey, & Evans, 1995; Urgesi, Calvo-Merino, et al., 2007; Wolpert, Goodbody, & Husain, 1998). Thus, while both visual streams process information that could potentially inform the prospective analysis of biomechanical viability, it is unclear whether the actual selection of comfortable hand postures depends on the ventral or dorsal stream, or some combination of the two.

An effective way of studying postural decision-making is to measure manual bistability during a grasping task (Bardy, Oullier, Bootsma, & Stoffregen, 2002; Buchanan, Kelso, & Fuchs, 1996). While the perceptual bistability we experience during binocular rivalry or when we look at ambiguous figures (such as the Necker cube or the Rubin vase) is the result of a single sensory stimulus being placed into two perceptual categories (Leopold & Logothetis, 1999; Sterzer, Kleinschmidt, & Rees, 2009), postural bistability results instead from a single perceptually unambiguous stimulus eliciting two mutually exclusive grasp postures. In the past, we have called this "motor ambiguity" (Wood & Goodale, 2011). Within a bistable state, a final grasp selection is more likely to be influenced by the subtler influences of variables like hysteresis (Kent, Wilson, Plumb, Williams, & Mon-Williams, 2009), visual context (Crajé, van der Kamp, & Steenbergen, 2008; Dyde &

Milner, 2002; Glover, Dixon, Castiello, & Rushworth, 2005), and starting hand position (Dijkerman, Mcintosh, Schindler, Nijboer, & Milner, 2009). In this sense, the factors that guide postural decision-making are amplified when the relevant behavior is bistable.

A recent study showed that two patients (SB and DF) with bilateral lesions to the lateral occipital area (LO) lacked an anticipatory appreciation of the biomechanical constraints for grasp posture choices, as evidenced by bistability (operationalized as postural variability during a grasping task) over a broader range than in neurologically intact participants. The authors concluded that sensitivity to these constraints depended on a perceptual analysis of relevant object features by the ventral stream (Dijkerman et al., 2009). However, it is now known that the two patients studied, known as DF and SB, also suffer from dorsal stream pathology. In particular, a recent analysis of DF's brain indicates that she has significant cortical thinning in the posterior extent of the intraparietal sulcus (IPS) (Bridge et al., 2013). It is possible that the impaired grasp posture selection in both DF and SB was due to dorsal rather than ventral stream pathology. Consistent with this proposal, functional magnetic resonance imaging (fMRI) results from imagined prehension tasks show that the posterior aspects of the IPS (pIPS) and the superior parietal lobule (pSPL), putatively encompassing the human Brodmann area 7, mediate upper limb postural decisions based on anticipated biomechanical constraints (Johnson et al., 2002; Zimmermann, Meulenbroek, & de Lange, 2011). Thus, it is still unclear whether these patients' deficits were due to their ventral or dorsal stream lesions.

In the present investigation, a cohort of neurologically intact participants and two brain-damaged patients selected one of two possible postures (thumb-left or thumb-right; Fig. 1) for grasping a bar at various orientations (Kelso, Buchanan, & Murata, 1994; Stelmach, Castiello, & Jeannerod, 1994). At most orientations, the biomechanical costs (i.e., limb rotation) for the two grasp postures were quite different and the bar afforded a stable preference for just one of the two postures. At some orientations, the limb approached the limits of rotation for both postures, resulting in more variable posture selection due to manual bistability. The patients had bilateral LO lesions and either bilateral (patient DF) or unilateral (patient MC) pIPS/pSPL lesions. This pattern of lesions—in particular, the unilateral nature of MC's parietal lesion—enabled us to test whether the selection of biomechanically viable postures is mediated by LO, pIPS/pSPL, or both areas.

In a separate fMRI experiment, a different cohort of neurologically intact participants performed a similar hand posture selection task while we measured the blood-oxygen-level dependent (BOLD) response. Given the evidence that behavioral bistability is accompanied by competition between mutually exclusive neural states (Blake & Logothetis, 2002), which results in a higher BOLD response (Durston et al., 2003), we modeled the BOLD response as a linear function of manual bistability. This revealed a cortical network, including pIPS/pSPL (overlapping with the patient lesions), where BOLD modulation was correlated with manual bistability. Together, the lesion-deficit and imaging results presented here provide evidence that pIPS/pSPL is critical for the selection of biomechanically viable grasp postures.
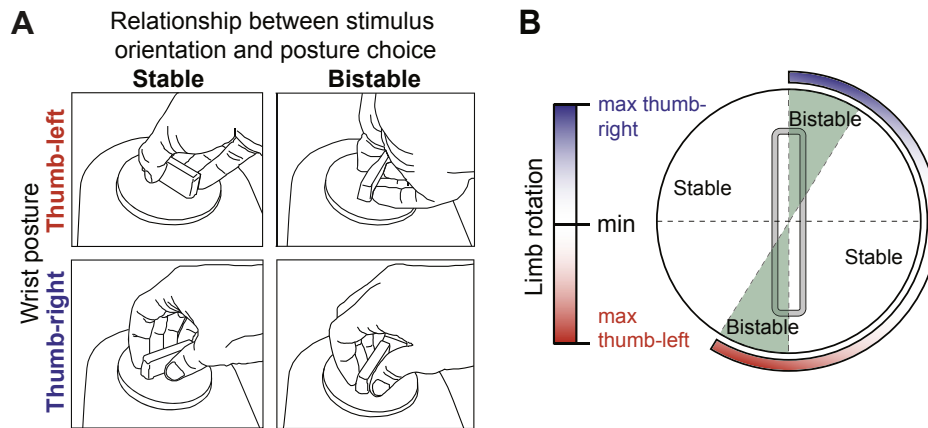
Fig. 1 — Bistability in grasp postures. (A) Depiction of typical postures for orientations where posture selection is either stable or bistable. (B) A depiction of typical bistable (green) and stable (white) object orientations in the fMRI task. The range of bistable orientations is approximately specified by the overlap between the respective limits of thumb-right (blue) and thumb-left (red) rotation.

2. Methods

This study consisted of two experiments: (1) a behavioral experiment performed on two brain-damaged patients (DF and MC) and a cohort of neurologically intact control participants, and (2) an fMRI experiment carried out in a separate group of neurologically intact participants (Fig. 2). The goal of the behavioral experiment was to determine the effects of damage to the ventral and dorsal streams on the selection of biomechanically viable grasp postures. The goal of the fMRI experiment was to determine whether or not group-level activation in the general population would overlay, in standardized stereotaxic space, specific brain lesions in the patients. Informed consent was obtained according to procedures and protocols approved by the Health Sciences Research Ethics Board at The University of Western Ontario.

2.1. Participants

2.1.1. Participants: behavioral experiment
Two brain-damaged patients participated in this experiment. Both patients had average levels of intelligence (Dutton, 2003; Goodale, Milner, Jakobson, & Carey, 1991; Goodale et al., 2008; Wolf et al., 2008). We also tested two separate groups of neurologically intact control participants. The first group, consisting of eight participants, was not age-matched (AM) (three females; age range, 22—36 years old; mean age, 27.8). The second group, consisting of 10 participants, was AM (five females; age range, 39—69 years old; mean age, 56.7). Handedness was assessed through self-report (Edinburgh Handedness Inventory, Oldfield, 1971). The non-age-matched (NAM) control group were all right-handed. The AM control group had three left-handed and seven right-handed participants. However, there were no differences in performance between left- and right-handed participants (*p* > .2), so we made no distinction between them during analysis. All control participants reported normal or corrected-to-normal visual acuity.

DF: After suffering from carbon monoxide poisoning in 1988, DF developed extensive bilateral lesions in LO and small bilateral lesions in the superior parietal cortex. As a result of her LO lesions, she was diagnosed with visual form agnosia (Goodale et al., 1991). We tested DF in 2009 (right and left hand). However, we did not fully trust the data from her left-hand performance because it appeared to be out of the optimal range for testing, as evidenced by the fact that she selected the same posture on all but three trials. Therefore, we tested DF again in 2013, focusing only on her left-hand performance. She was 53 and 57 years old, respectively, at the times of testing. The task was identical on both occasions. DF is right-handed (Goodale et al., 1991).

MC: MC was 30 years old when she contracted a severe respiratory infection. A resulting stroke left her with extensive bilateral lesions in the occipitotemporal cortex. The majority of her primary visual cortex (V1) was compromised, leaving her cortically blind in static perimetry, and with only a small spared patch of motion sensitivity in the upper left quadrant of her visual field (Dutton, 2003). MC also has bilateral lesions to area LO and a right-hemisphere lesion in the posterior parietal cortex. In spite of this extensive damage to V1 and other visual regions in occipital and temporal cortex, MC has displayed a preserved ability to perform visually guided movements (Goodale et al., 2008; Wolf et al., 2008). The exact source of these preserved abilities is not currently known. She was born in 1969, and we tested her in 2009, making her 40 years old at the time of testing. MC reported being right-handed (Edinburgh Handedness Inventory, Oldfield, 1971).

2.1.2. Participants: fMRI experiments
Fifteen right-handed participants (nine females; age range, 19—31 years old; mean = 23.6) reporting normal or corrected-to-normal visual acuity, intact color vision, and no history of neurological impairments participated in the fMRI experiment on manual bistability. Thirteen of these participants (eight females; age range, 19—31 years old; mean = 23.8) also participated in two secondary localizer experiments that were designed to functionally define LO, pIPS/pSPL, and the dorsal premotor area (PMd) for the purposes of creating regions-of-interest (ROIs). None of the participants in the fMRI experiment participated in the behavioral experiment.
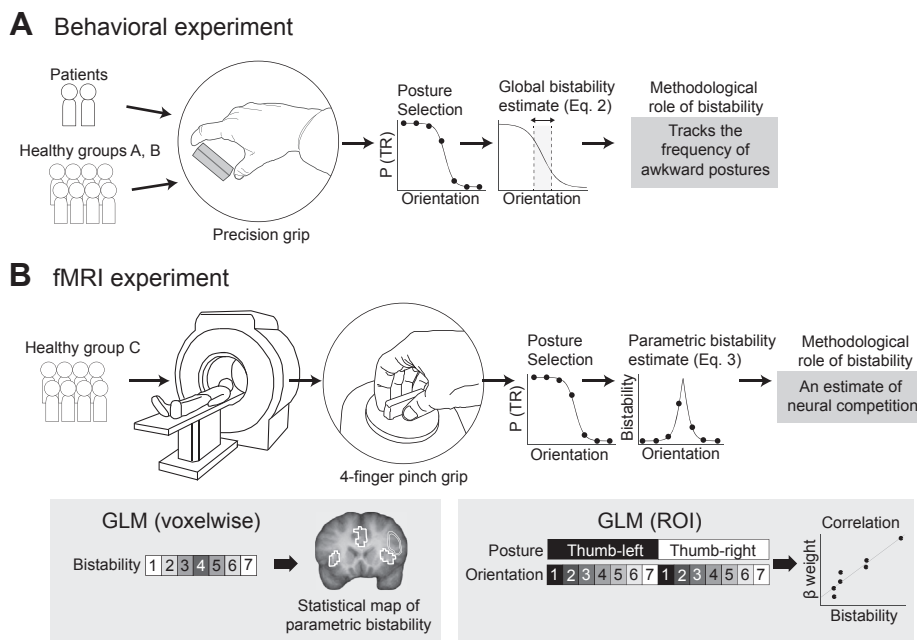
Fig. 2 — Experiments and analyses. (A) Behavioral experiment. Participants used a precision grip (i.e., forefinger and thumb only) to grasp a triangular cross-section bar at its ends. Bistability, estimated from postural choices, was used as an index of pathological postural decision-making. (B) fMRI experiment. Participants grasped an "oven dial" bar with the thumb on one side and the other four fingers on the other side. Bistability, estimated from grasp choices in the scanner, was used as an index of neural competition. Bistability was explicitly used as a predictor in the GLM for the whole-brain analysis, while it was tested for correlations with betas (derived from a GLM with posture and orientation as predictors) for the ROI analysis.

2.2. Procedures

2.2.1. Procedures: behavioral experiment

Both patients and the two groups of control participants performed a wrist posture selection task that involved reaching and grasping a wooden, triangular-section prism block by placing the thumb and index finger on opposite ends (Stelmach et al., 1994). The stimulus was presented in the horizontal plane, resting on the surface of a table. We manipulated the orientation of the stimulus and categorized posture selection as either thumb-left or thumb-right, depending upon which side of the stimulus the thumb was located.

Trials started with the fingers pinched together and resting on a release button located 10 cm from the table edge closest to the participant. The center of the stimulus was located 30 cm from the release button. Visual feedback of the stimulus was withheld between trials by liquid-crystal display goggles (PLATO; Translucent Technologies, Toronto, ON, Canada). A trial began when the goggles became translucent. Participants were instructed to reach out and grasp the stimulus as quickly and accurately as possible. Reaches were classified as errors if the first contact between the fingers and the stimulus was not on the specified ends of the stimulus.

Prior to testing, each participant completed a brief version of the task to provide us with an initial estimate of postural preferences. We then rotated the range of stimulus orientations so that the center orientation was most likely to produce the highest variability in posture selection (e.g., roughly half of the postures were thumb-left and half were thumb-right). Accordingly, all orientations were relative to the preferences of the individual participant.

This procedure was performed for both the right and left hand in separate blocks for each participant and patient. These data were typically collected on the same day, with the exception of DF, whose left-hand data were re-collected 4 years after her original testing. Since we do not compare performance between hands within the patients, the gap in testing between DF's right and left hands does not impact our interpretation of the results.

2.2.2. Procedures: fMRI grasping experiment

A different group of neurologically intact volunteers performed the wrist posture selection task during fMRI. The two patients did not participate in the fMRI experiment. Participants lay on the bed of the scanner with their head tilted forward 30°. This allowed a direct view (i.e., no mirrors) of an apparatus in which the stimulus (an elongated dial) could be presented in seven different orientations, each separated by 10°. Unlike the stimulus in the behavioral experiment, which was oriented in the horizontal plane, the dial was oriented in the frontal plane. Participants were instructed to grasp the dial with the right-hand thumb on one side, and the four other fingers on the opposing side (i.e., a pinch grip). To minimize reach-related movement artifacts, we strapped down the participants' right arms at the lower bicep. This had little impact on the wrist abduction and supination required for thumb-left postures, but it inhibited the characteristic thumb-right posture, which consists of adduction and pronation of the wrist and abduction of the arm. This had the effect of truncating the range of comfortable rotation only for thumb-right postures. Given that we later derived bistability estimates from the behavior in the scanner, we were able to relate

behavior directly to the neural response without worrying about how participants might have performed in an unconstrained environment.

After immobilizing the arm, but prior to inserting the participant into the scanner bore, we adapted two parameters of the stimulus to the participant. First, the distance of the stimulus was matched to the range of the participant's reach. Second, we used a short staircase procedure to identify the stimulus orientation where posture selection was most variable, and then shifted the seven possible stimulus orientations so that the highest variability occurred at the central orientation. This was done to ensure that the stimulus orientations for each participant were relative to the metrics of that participant's limb. Accordingly, all further references to the stimulus orientation in the fMRI experiment should be understood as relative, not absolute, orientation.

The fMRI experiment had a slow event-related design. Testing was carried out in complete darkness. Prior to each trial, a light behind the stimulus platform briefly illuminated a rear-facing stimulus handle, allowing the experimenter to change the orientation of the stimulus without visual feedback to the participant. The stimulus was rotated to one of seven different orientations in a pseudo-random order. Throughout the experiment, participants fixated on an LED just above the stimulus. Each trial began with a light illuminating the stimulus for 200 msec. This served as a go-cue to reach out, grasp the stimulus, and return the hand to its starting position. The entire movement lasted 2 sec at most. Under these brief viewing constraints (i.e., 200 msec), different eye-gaze strategies across different orientations would not be advantageous, if at all possible, to perform.

Using an MRI-compatible infrared video camera (MRC Systems, Heidelberg, Germany) to record each participant's performance, we categorized wrist postures as either thumb-left or thumb-right, referring to the position of the thumb on the stimulus. No other behavioral measures were collected. For experimental control, we used a custom software program written in the Psychophysics Toolbox extension (Brainard, 1997) for Matlab (MathWorks, Inc., Natick, MA, United States). The fMRI experiment consisted of 10 runs with 232 volumes in each run. Each run consisted of 30 trials, with each trial lasting 14 sec.

2.2.3.   Procedures: fMRI localizer experiments

We also carried out two additional fMRI experiments in order to functionally define ROIs. In these experiments, we used E-Prime 2.0 (Psychology Software Tools, Pittsburgh, PA, United States) to present stimuli on a screen in the back of the scanner. Participants viewed the stimuli via a mirror attached to the head coil. Participants maintained fixation on a small dot in the center of the screen. On a given block, 12 stimuli were presented for 600 msec each followed by a blank image for 150 msec. Each block was followed by a 9 sec delay before the start of the next block. For both localizers, we carried out two runs of 116 volumes. There were nine blocks for each condition per run. Of the original 15 participants in the fMRI grasping experiment, we were able to bring 13 back to participate in these localizer experiments at a later date.

The first localizer experiment aimed to functionally define LO and pIPS, both of which should be engaged when simple

geometrical shapes are presented at different orientations (Bonda et al., 1995, 1996; Silson et al., 2013; Urgesi, Calvo-Merino, et al., 2007; Valyear, Culham, Sharif, Westwood, & Goodale, 2006; Wolpert et al., 1998). We presented different orientations of intact and scrambled images of elongated novel objects (taken from: http://wiki.cnbc.cmu.edu/Novel_Objects). These images were presented in gray-scale format and subtended 6.5° in visual angle. Subtracting the BOLD response to their scrambled configurations from their intact configurations enabled us to define ROIs for LO as well as an area slightly more dorsal to the pIPS in the SPL, which we will refer simply as pSPL.

The second localizer experiment aimed to functionally define PMd, which is typically engaged when people perform a choice reaction task based on learned paired associations with arbitrary sensory cues (Chouinard & Goodale, 2009; Chouinard & Paus, 2010). We modified an approach that was first developed by Amiez, Kostopoulos, Champod, and Petrides (2006). Participants pressed a specified response button whenever the screen turned a different color (Multiple Response). Specifically, participants pressed button 1 for red, button 2 for yellow, button 3 for green, and button 4 for blue. In a different condition, participants made the same response to the repeated presentation of the same color (Single Response). Subtracting the Single Response condition from the Multiple Response condition enabled us to define ROIs in the premotor cortex (PMd) (Chouinard & Paus, 2006; Picard & Strick, 2001).

2.2.4.   Procedures: acquisition of the MRI data

Scanning was performed on a 3-T Tim Trio Siemens MRI system with the posterior half of a 12-channel receiver-only head coil (six channels) to cover the back of the brain and a 4-channel flex coil to cover the front of the brain. An anatomical scan was performed encompassing the whole brain. This was achieved by collecting 192 1-mm-thick slices using a 3D T1-weighted acquisition sequence (TI = 900 msec, TE = 3.43 msec, TR = 2300 msec, flip angle = 9°). The in-plane resolution of the anatomical scans was 256 × 240 pixels.

To collect the functional data for the fMRI grasping experiment, we used a T2*-weighted echo-planar imaging sequence (TE = 30.0 msec, TR = 2000 msec, flip angle = 90°). The field of view was 24.0 × 24.0 cm with an in-plane matrix size of 80 × 80 pixels. Each image covered the whole cortex and consisted of 34 slices (voxel size = 3.0 × 3.0 × 3.5 mm) that were oriented in the same plane as the AC–PC plane.

Functional data for the localizer experiments were collected using a T2*-weighted echo-planar imaging sequence (TE = 30.0 msec, TR = 3000 msec, flip angle = 78°). The in-plane matrix size was 80 × 80 pixels with a field of view of 16.8 × 16.8 cm. Each image encompassed the whole cortex and was composed of 42 slices oriented parallel to the AC–PC plane (isotropic voxel size = 3.0 mm). There were no gaps between slices for any of the experiments.

2.2.5.   Procedures: preprocessing of the MRI data

All imaging data were preprocessed using Brain Voyager software (BV QX 2.4, Brain Innovation, Maastricht, The Netherlands). For each participant, functional data from each session were screened for motion artifacts. After confirming that head motion did not exceed 1 mm translation or 1°

rotation, we performed motion correction, then slice-time correction, then spatial smoothing, and then spatial normalization. We note here that smoothing before normalization made no difference in our results; all observed effects remained the same when we performed the analysis after having normalized prior to smoothing. Motion correction was carried out using the trilinear 3D sinc algorithm to align all functional volumes to the third volume of the first run. The first two volumes in each run were excluded because they might not be representative of steady state. A slice-time correction algorithm was used to correct for differences in acquisition times between slices. Drift was removed using an algorithm that removes linear trends and a high-pass filter was applied to remove temporal frequencies below two cycles per run. A Gaussian filter was used to achieve a final 8-mm full-width half-maximum of smoothing in the data after re-interpolating the data to an isotropic voxel size of 3.0 mm. Finally, all images were linearly transformed into Talairach space. This spatial normalization enabled us to ensure that all MRI data were in the same space across participants and the different fMRI experiments that were performed. In addition, it enabled us to also make comparisons between the spatial location of activation in the neurologically intact participants and the lesions shown in the anatomical scans of DF and MC.

2.3. Analysis

2.3.1. Analysis: data acquired during the behavioral experiment
Posture selection during the experiment was coded with respect to the position of the thumb relative to the stimulus. Wrist postures where the thumb touched the left side of the bar were classified as *thumb-left* and those where the thumb touched the right side were classified as *thumb-right* (Fig. 2A). The probability P of using a thumb-right posture at orientation x was described by the logistic function:

$$P(x) = \left(\frac{e^{b_0 + b_1 x}}{1 + e^{b_0 + b_1 x}} \right) \tag{1}$$

where b_0 and b_1 are coefficient estimates based on an initial general linear model (GLM) (binary logit) fit. We then calculated the manual bistability width ω of a participant's performance as:

$$\omega = P_{25} - P_{75} \tag{2}$$

where P_{25} and P_{75} are estimates of the orientation at which P is equal to the 25th and 75th percentile of thumb-right posture probability, respectively (Fig. 4B). This measure is proportional to the number of orientations where subjects were variable in their posture selection. We used this measure of manual bistability width to quantify posture selection deficits in the patients. Using a *t*-test modified for comparing single cases with a control group, we tested for behavioral dissociations between the two patients and a group of healthy controls (Crawford, Garthwaite, Howell, & Gray, 2004). Here, and for all other analyses, we used the Bonferroni method to correct for multiple comparisons, and set alpha at *p* < .05.

We tested DF and MC twice with the left hand (DF in 2009 and 2013, and MC in 2009 during a single session). This was due to the fact that, in the first run with the left hand, both patients selected the same posture on virtually every trial (Fig. 4B), making any estimates of bistability somewhat arbitrary. To test our suspicion that we had merely tested them at an extended range where biomechanical constraints for the two postures did not overlap, we tested them in a different range of orientations and found a more traditional, although impaired, pattern of behavior (Fig. 4A). Although the performance in the first left-hand runs precluded any analysis of bistability width, we report the presence of these data for completeness.

2.3.2. Analysis: behavioral data acquired during the fMRI grasping experiment
Wrist postures were redundantly coded by two of the authors (D.K.W. and A.J.M.) offline from the video recordings. Trials in which the thumb touched the left edge of the dial were coded as *thumb-left* and trials in which the thumb touched the right edge of the dial were coded as *thumb-right*. For each participant, we used Eq. (1) to calculate the probability P of using a thumb-right wrist posture at each orientation. We then calculated an index of bistability, B, for each orientation x, using the following equation:

$$B(x) = 2(||P(x) - .5| - .5|) \tag{3}$$

Here, we essentially folded P at .5 and multiplied this by 2 so that the maximum was 1 and the value of B at any given orientation was proportional to the estimated variability of the wrist posture. This bistability index was then used as a predictor of BOLD activity during the fMRI analysis.

2.3.3. Analysis: whole-brain approach for the fMRI grasping experiment
A GLM was used to analyze the BOLD signal. The data were first analyzed at the subject level. Three types of predictors were incorporated in the model. The first predictor was a stick function that was not convolved with any kind of hemodynamic response function. This predictor was placed at the first volume of each trial in order to account for the variance driven by any sudden head movements conducted by shoulder movements during reaches, which typically looks like a spike in the BOLD signal. This approach in dealing with head movements during reaches in slow event-related designs has been validated and described in more detail elsewhere by researchers who pioneered the use of reaching behavior in fMRI studies (Culham et al., 2003). The second predictor modeled the effects of task. This predictor was convolved with a standard double-gamma hemodynamic response function for each trial. The third predictor parametrically modeled the effects of manual bistability on the BOLD signal. This predictor was created by convolving the latter predictor with the value of B [Eq. (3)] at each orientation. We then carried out a second level of analysis that incorporated the data across all subjects using a random effects model to test for significant effects of the third predictor at the group level. To assess significance, we performed a cluster analysis to correct for multiple comparisons in a brain volume of 1000 cm^3 using procedures based on random field theory described by Worsley, Evans, Marrett, and Neelin (1992). The *t*-statistical map resulting from this analysis was superimposed over the average

anatomical MRI of all participants. When completed, the analysis allowed us to assess the degree to which the mid-to-late components of the BOLD response were parametrically modulated by manual bistability.

2.3.4. Analysis: defining ROIs from the fMRI localizer experiments

Data from the fMRI localizer experiments were first analyzed at the subject level using a GLM in the following manner. For each localizer experiment, separate predictors for the two conditions were convolved with a standard double-gamma hemodynamic response function. We then determined the *t*-statistic at every voxel for Intact Objects > Scrambled Objects in the LO/pSPL localizer experiment, and Multiple Choice Responses > Single Choice Response for the PMd localizer experiment. While defining ROIs for each of these brain areas, the *t*-statistical maps were superimposed with the individual's anatomical MRI. We selected the 10 most significant contiguous voxels to create ROI masks while considering the following anatomical criteria: all ROIs for LO were located in or near the lateral occipital sulcus, all ROIs for pSPL were in the posterior portion of the SPL either along the dorsal bank of the IPS or along the outer surface of the cortex, and ROIs for PMd were typically located in its caudal subdivision, posterior to the junction of the precentral and superior frontal sulci. For this reason, we will denote this ROI from now on as caudal premotor dorsal area (PMdc). We also assessed significance at the group level by carrying out a second level of analysis that incorporated the data across all subjects using a random effects model. To assess significance at the group level, we established cluster thresholds using the same procedures as those described earlier for the fMRI grasping experiment.

2.3.5. Analysis: ROI approach for the fMRI grasping experiment

An ROI approach was used to examine the effects of both bistability and limb rotation (i.e., biomechanical costs) on brain activation. Data were entered into a GLM that differed from the one described earlier for whole-brain analysis. In this GLM, we included 14 predictors of interest, each one corresponding to one of two grasp postures that was selected at one of the seven different orientations. After creating this GLM separately in each individual, we then extracted the beta weights for each of the different orientations for when *thumb-left* was selected and for when *thumb-right* was selected (using the non-parametrically weighted estimates). Pearson's *r* was calculated between beta weights and manual bistability for each participant. After doing this in all participants, we used Bonferroni corrected *t*-tests to test whether the average correlation for each ROI was different from zero. For plotting purposes, we then bootstrapped (random sampling with replacement) an estimate of the median correlation across participants, along with 99% confidence intervals (10,000 iterations). We excluded from this analysis any conditions where the beta estimate was the result of only one trial (e.g., where thumb-left posture was only used once at a particular orientation). This was done under the assumption that an estimate based on one observation is unreliable in a signal as variable as the BOLD signal. This resulted in less than 1% of trials being discarded. We also excluded one participant from

the analysis due to a failure on the part of the experimenter to accurately estimate the participant's preferred orientation for switching between postures, prior to the experiment. This resulted in the participant having a manual bistability function with a peak at one of the extreme orientations rather than near the central orientation.

2.3.6. Analysis: defining lesions in DF and MC

We carried out a lesion analysis with the MINC tools package (http://www.bic.mni.mcgill.ca/ServicesSoftware/MINC). After the anatomical images of DF and MC were corrected for intensity non-uniformity, the lesions were manually defined and segmented. For every slice along the sagittal, coronal, and transverse planes, a range of intensities was customized for each patient so that the segmenting would encapsulate pathological as opposed to intact tissue. After this manual segmentation procedure, an aggregated image of both the anatomical and lesion images was created (i.e., an anatomical MRI in which the lesions were filled in) and used to create a transformation matrix from native-to-MNI space (Collins, Neelin, Peters, & Evans, 1994). This approach of aggregating the two images simulated an intact brain, which helped contribute to the accurate spatial normalization transformation matrices for the two patients. We then used these transformation matrices and the MNI template brain to resample the anatomical and lesion-defined images from native-to-MNI space separately (Collins et al., 1994). Finally, we transformed the coordinates of activation from Talairach to MNI space using an algorithm developed by Dr. Matthew Brett (http://imaging.mrc-cbu.cam.ac.uk/imaging/MniTalairach) and superimposed the MRI of both patients, the lesion images of both patients, and the location of group-level activation from the fMRI experiment. These spatial normalization procedures allowed us to make comparisons between the spatial locations of the activation acquired in the fMRI experiments in the neurologically intact participants and the spatial locations of the patients' lesions.

3. Results

3.1. Posture selection deficits in patients DF and MC

Our initial goal was to test whether the excessive bistability in grasp posture selection observed in earlier patient studies (Dijkerman et al., 2009) is due to ventral or dorsal stream pathology (Fig. 3). We compared the performance of two healthy control samples against two patients with different patterns of lesions in the ventral and dorsal streams. The first control sample was not AM to the patients. Therefore, to ensure that any deficits in the patients were not due to age, we also collected an AM sample. There were no differences in performance between the two control groups (i.e., age had no effect on the selectivity of posture selection, $p > .2$ for both hands) so we collapsed them into one group before comparing them with the patients.

With her right hand, DF (who has bilateral ventral and dorsal stream lesions) had a wider manual bistability range ($\omega = 14.42°$) compared to controls ($\omega = 4.45° \pm 3.11$ SD), $t(17) = 3.12$, $p < .01$. DF's left-hand performance was also
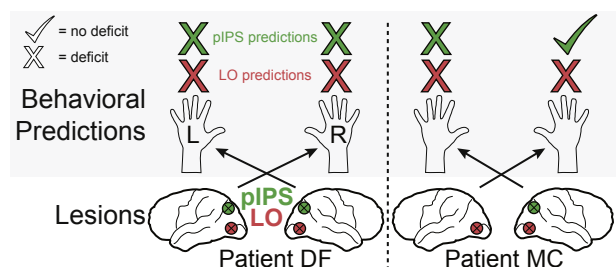
Fig. 3 — A depiction of the sites of relevant cortical lesions in patients DF and MC, and behavioral predictions if the ventral (red) or dorsal (green) visual streams are necessary for using visual object orientation to inform biomechanically viable postures during reach-to-grasp movements.

impaired (ω = 19.45°) compared to healthy controls (ω = 5.49° ± 3.59 SD), $t(17)$ = 3.78, p < .001. Note that, considered in isolation, DF's bilateral impairment in grasp posture selection could be due to her bilateral lesions in either LO or pIPS/pSPL, or some combination of the two. In other words, the case of DF, considered in isolation, cannot shed light on the relative contributions of the ventral and dorsal streams to the behavior of using visual feedback to select a comfortable grasp posture. However, we also report the performance of MC, who has extensive bilateral lesions to the ventral stream (including LO) and a right-hemisphere lesion in pIPS. Critically, her left-hemisphere posterior parietal cortex is intact. Left-handed posture selection (i.e., contralateral to the lesioned pIPS/pSPL) in MC was severely impaired (ω = 32.28°) relative to controls, $t(17)$ = 7.25, p < .0001. However, right-handed performance (i.e., contralateral to intact pIPS/pSPL) in MC (ω = 1.37°) showed sensitivity rivalling the best performance in healthy controls (Fig. 4A—C), $t(17)$ = −.97, p = .35. This result suggests that the integrity of contralateral pIPS/pSPL plays a causal role in the selection of comfortable grasp postures.

Even though we collapsed the two control groups before comparing them with the patients, we note here that the results were not affected by keeping the control groups separate. Similar to the statistics of the collapsed comparison, bistability widths in both groups were significantly different from the patients in all conditions except for one: MC's right-hand performance was not different from right-hand performance in either of the two control groups.

Despite impaired grasp posture selection, the patients still accurately scaled their hand and fingers to the bar orientation. Accurate grasping and scaling of the wrist is well documented in DF (Dijkerman et al., 2009; Goodale et al., 1991). MC also displayed accurate grasping (Fig. 5A). The rare fumble or drop occurred almost exclusively in cases where the patient attempted to use an awkward posture that was at or beyond the limits of possible wrist rotation (Fig. 5A, B).

We also tested for effects of manual bistability on reaction time (RT). For control participants (NAM), bistability and RT (collapsed across right and left-handed performance since there were no differences between them) were positively correlated, r = .46, p < .05. This replicates previous findings (Wood & Goodale, 2011). There was no significant relationship

between manual bistability and RT for DF and MC (p > .05), both within and across hands.

3.2. fMRI experiment: whole-brain analysis

A whole-brain voxel-wise analysis revealed that manual bistability parametrically modulated dorsolateral prefrontal cortex (DLPFC), ventrolateral prefrontal cortex (VLPFC), the more rostral subdivision of PMd (PMdr; Chouinard & Goodale, 2009), and parietal cortex, including pIPS (Fig. 6; see Table 1). There was no parametric BOLD modulation in the ventral stream, including LO, which suggests that a perceptual analysis of object shape and orientation is not required to select a biomechanically informed wrist posture in our task. Further, there was no significant motor cortex activation (Fig. 6F), which suggests that the parametric activation observed in our analysis was not merely a function of motor execution.

3.3. ROIs defined from the fMRI localizer experiments

Ventral stream contributions to posture selection, if present, may have been too subtle for a whole-brain voxel-wise analysis, especially given both the conservative nature of this analysis and the problem of anatomical variability in sulcal anatomy in standardized Talairach space. To improve sensitivity, we re-examined the functional data within ROIs that were functionally defined in separate localizer experiments, which were robust enough to define LO, pSPL, and PMdc bilaterally in all participants. A whole-brain voxel-wise analysis revealed how each of our ROIs reached significance at the group level (Table 2). We observed some spatial discrepancies in the precise X, Y, and Z coordinates for the peak activation obtained between the fMRI experiments (Tables 1 vs 2; see also Fig. 9). Specifically, PMd tended to be engaged in a more rostral subdivision in the fMRI grasping experiment relative to the PMd localizer experiment (Euclidean distance = 12.37 mm) while pIPS/pSPL tended to be engaged more inside the depths of the IPS in the fMRI grasping experiment relative to the LO/pSPL localizer experiment (Euclidean distance = 16.16 mm). We have therefore provided slightly different nomenclatures (e.g., PMdr and PMdc for the rostral and caudal subdivisions of the dorsal premotor cortex) between experiments to better characterize the spatial location of our findings.

3.4. fMRI experiment: bistability, not limb rotation, drives parametric activation

Results obtained from the ROI analysis were similar to those obtained from the whole-brain analysis. Here, we report the mean correlation between beta estimates (derived from a GLM with orientation and posture as predictors) and bistability at each orientation, as well as p values from t-tests that tested whether the distribution of correlations was different from zero. As shown in Fig. 7A, BOLD activity was found to be parametrically modulated as a function of manual bistability in the left PMdc (*mean Pearson's r* = .57, p < .0001), the right PMdc (m = .38, p < .05), the left pSPL (m = .48, p < .005) and the right pSPL (m = .55, p < .001) but not in the left LO (m = .05, p = .86) or the right LO (m = .03, p = .92). We emphasize that the pSPL voxels, extracted from passive visual stimulation alone
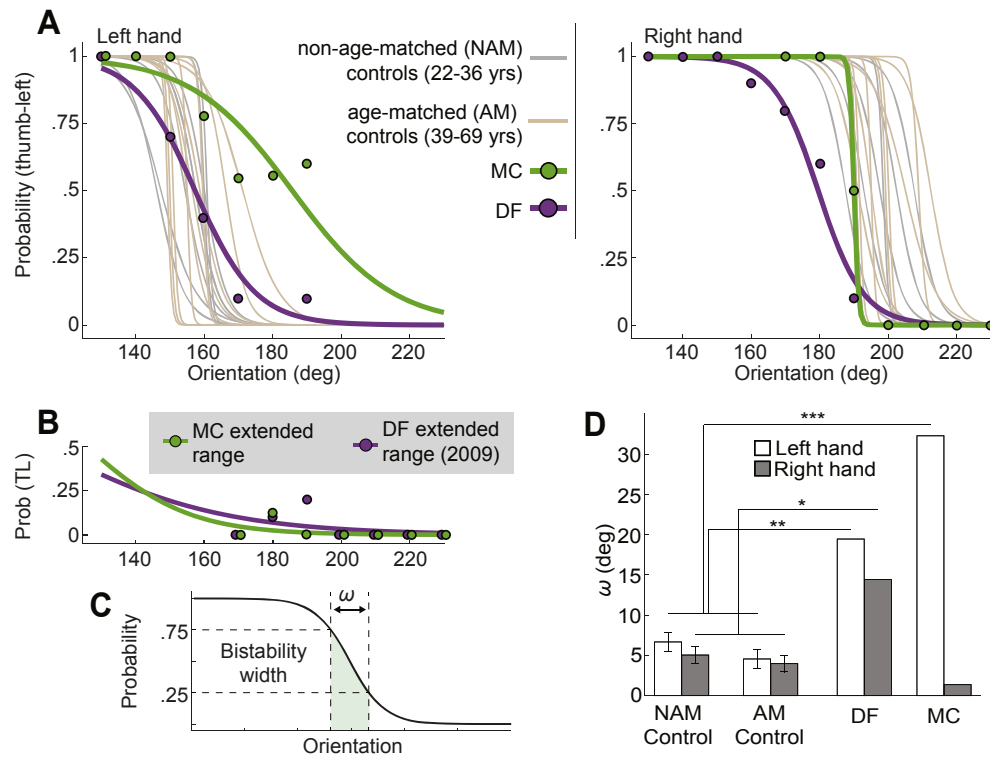
Fig. 4 — Patient behavioral results. (A) Posture selection and logistic fits for left- and right-hand performance in patients and controls. (B) Left-handed posture selection in the patients at an extended range. (C) Manual bistability range width (ω) is the difference in orientation between the 25% and 75% probabilities for selecting thumb-left. A larger ω value indicates higher frequency of awkward postures. (D) Average width of bistability range (ω) for controls versus patients DF and MC. $^{*}p < .05.$ $^{**}p < .01.$ $^{***}p < .001..$
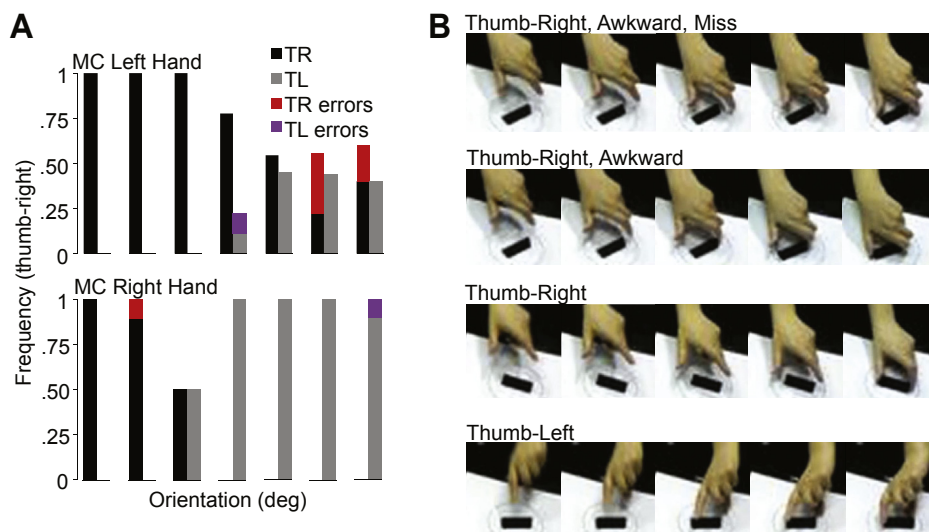

Fig. 5 — Preserved accuracy and impaired postural decision-making in MC's left-hand performance. (A) Grasp errors (i.e., first contact between fingers and object was not on specified edges of object) in the performance of patient MC. (B) Captured stills from footage of patient MC performing the task. Four different cases are depicted: (1) Bottom row: successful thumb-left, (2) Lower middle: successful thumb-right, (3) Upper middle: successful but extremely rotated thumb-right, and (4) Top: unsuccessful thumb-right, due to attempting a posture at the limits of arm rotation.
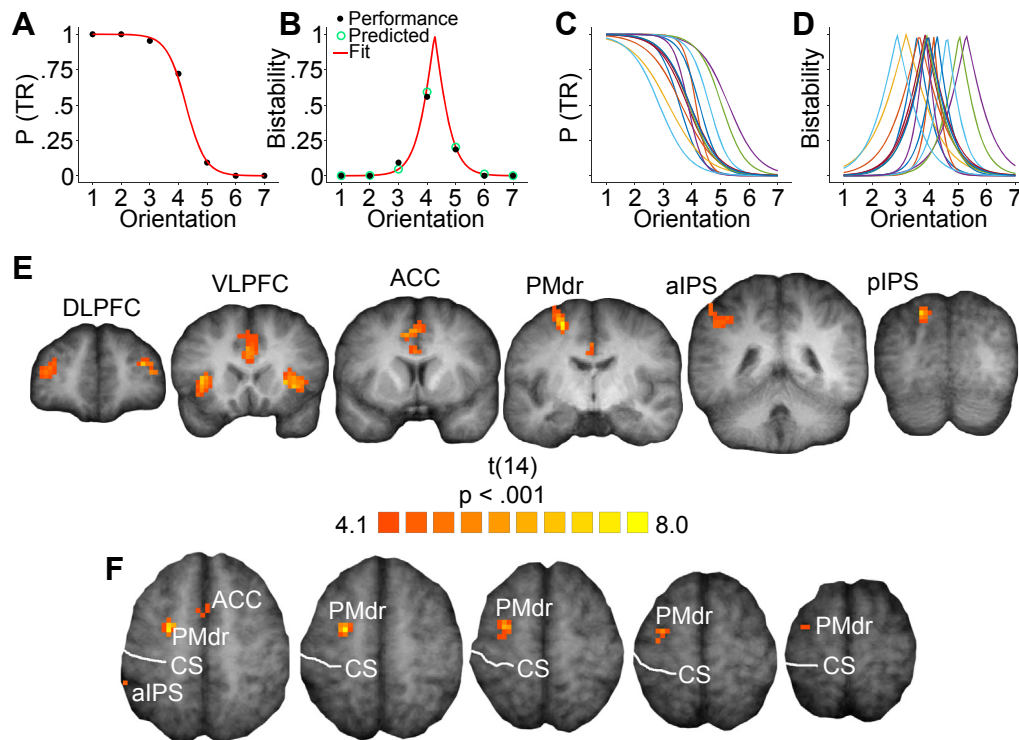
Fig. 6 — Voxel-wise fMRI results. (A) We fit logistic functions (red line) to average posture selection (black dots) in order to estimate probability of thumb-right posture, shown here for a single subject. (B) Predicted manual bistability values (green circles) at each orientation were extracted from the folded probability fit. (C, D) Probability and manual bistability estimates for the group. The predicted bistability scores at each orientation were used as a predictor for the GLM. (E) Voxel-wise parametric maps. See Table 1 for X, Y, Z coordinates, t-statistics, and cluster sizes. (F) Absence of significant parametric activation in motor cortex. Abbreviation: CS (central sulcus).

Table 1 — Results from the whole-brain analysis for the fMRI manual bistability experiment.

Brain area	Anatomical landmark	X	Y	Z	$T_{(14)}$	Cluster size, $p < .001$ (mm³)
Right VLPFC	Frontal operculum	32	16	3	6.8	2457
Left VLPFC	Frontal operculum	−34	16	6	6.9	1917
Right mid-DLPFC	Middle frontal sulcus	32	43	21	6.8	540
Left mid-DLPFC	Middle frontal sulcus	−31	40	27	6.5	1377
ACC	Anterior aspect of the cingulate sulcus	−4	13	24	6.5	4401
Left PMdr	Precentral sulcus near junction with superior frontal sulcus	−22	−8	51	8.2	1026
Left pIPS	Posterior, dorsal aspect of the IPS	−19	−71	39	7.1	972
Left aIPS	Anterior aspect of the IPS	−40	−47	36	5.0	1215

All coordinates are in Talairach space.

Table 2 — Localised ROIs at the group level that were derived from the fMRI localizer experiments.

| Brain area	Anatomical landmark	X	Y	Z	$T_{(12)}$	Cluster size, $p < .001$ (mm³)
A) Functional localizer 1 (LO, pSPL)						
Left LO	Lateral occipital sulcus	−43	−71	−3	11.7	8370
Right LO	Lateral occipital sulcus	41	−74	−6	9.1	5859
Left SPL	SPL, near or inside the posterior, dorsal aspect of the IPS	−25	−62	51	6.0	1944
Right SPL	SPL, near or inside the posterior, dorsal aspect of the IPS	23	−59	48	5.7	459
B) Functional localizer 2 (PMd)						
Left PMdc	Precentral gyrus near superior frontal/precentral sulci junction	−31	−14	57	7.8	6360
Right PMdc	Precentral gyrus near superior frontal/precentral sulci junction	29	−17	54	11.2	5859

All coordinates are in Talairach space.
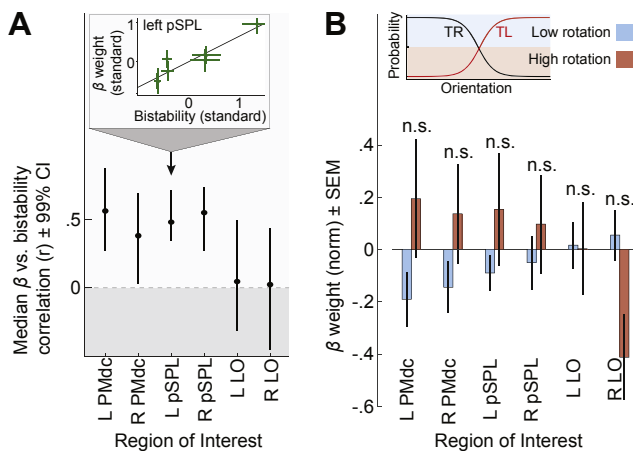
Fig. 7 – ROI analysis. (A) Bootstrapped median within-participant correlations between bistability and beta at each ROI. For illustration purposes, inset depicts correlation over average bistability and beta estimates for left pSPL. Error bars indicate 99% bootstrapped confidence intervals. (B) Where posture selection was variable, there was a trend of higher beta values for postures with a higher degree of limb rotation in the PMd and pIPS ROIs. However, none of the t-tests reached significance.

(see localizer task details in Methods), were modulated by manual bistability, which was a predictor derived from actual motor performance during the grasping task. This finding is consistent with the hypothesis that pSPL performs operations critical to the transformation of visual information into biomechanically sensitive plans for movement.

In our task, manual bistability was closely correlated with the degree of limb and wrist rotation (i.e., our operational definition of biomechanical cost) required to perform a grasp. Thus, our results could be driven by either manual bistability or limb rotation, or some combination of the two. Critically, these two variables tended to diverge in their predicted effects at orientations where both postures were used. At these orientations, the posture with the low probability requires more rotation, while the posture with the higher probability requires less rotation (Fig. 7B, inset), resulting in different predicted neural responses for the two postures. Meanwhile, since manual bistability is proportional to variability between postures, it is always the same for both postures at a given orientation, resulting in a prediction that there are no differences between neural responses for the two postures. We used t-tests to examine whether BOLD activity was different or the same between different levels of limb rotation within each ROI, but only at the orientations where the predictions of the two variables diverged for a given participant (i.e., at orientations where both postures were used and predicted limb rotation was not equal between postures). In PMdc and pSPL, there was a trend toward higher activation during more extreme limb rotation (Fig. 7B), but this trend was not significant in any of the ROIs ($p > .05$). This was true both when we collapsed across postures and when we tested them separately. Ultimately, our fMRI results appear to have been driven primarily by parametric manual bistability, but the trend of limb rotation suggests that biomechanical cost may also play a lesser role. And while our fMRI experiment was

driven by the hypothesis that parametric increases in manual bistability (as opposed to limb rotation) would isolate a network that included pIPS (based on our findings in MC and DF), we emphasize that the possibility that limb rotation was driving activation in our results is still consistent with a unique role of pIPS/pSPL in mediating postural decisions based on the knowledge of biomechanical constraints.

3.5. Spatial overlap between fMRI activation and patient lesions

To more directly relate the fMRI results with the outcome of the patient experiments, we superimposed the location of the fMRI results in the neurologically intact participants over anatomical MRI images (Fig. 8; whole-brain analysis only) and lesion maps (Fig. 9; whole-brain and ROI foci) of the two patients in standardized space. The only node in the parametric bistability activation network (from the fMRI grasping experiment) that overlapped with damaged tissue was the left pIPS/pSPL; all other areas of activation overlapped with intact cortical tissue in both patients. Importantly, the left pIPS/pSPL foci spatially corresponded to damaged tissue in DF and healthy tissue in MC. This is consistent with the impaired performance of DF and the intact performance of MC with the right hand. Right parietal lesion sites were homologous with the left pIPS/pSPL foci. This is consistent with the impaired performance of both patients with the left hand. Thus, combined with the pattern of behavioral deficits observed in DF and MC, these results provide converging evidence that when the contralateral pIPS/pSPL is damaged, it compromises the integrity of a cortical network that mediates postural decision-making, resulting in postures that betray an ambivalence to postural costs.

3.6. Task compatibility between the behavioral and fMRI experiments

The version of the task that was performed in the fMRI experiment differed from the one performed in the behavioral experiments. In the behavioral experiments, the participants placed their fingers at ends of the bar with their index finger and thumb and they did this sitting down at a desk (Fig. 2A). Conversely, in the fMRI experiment, the participants grasped the bar with the thumb on one side and the other four fingers on the other side and they did this lying down on the bed of a scanner (Fig. 2B). To test whether or not these differences influenced bistability scores, we carried out a control experiment comparing performance between the two variants of the task in 10 neurologically intact participants. The participants grasped the bar at the ends while sitting down in one condition and grasped the bar on either sides of the bar while lying down in the other condition. There was no difference between bistability scores in the two conditions, $t(9) = 1.02$, $p = .34$. This suggests that the dependent variable of interest, bistability, was unaffected by the added constraints of the fMRI task.

4. Discussion

We used neuroimaging and behavioral experiments to test whether the anticipation of limb posture awkwardness during
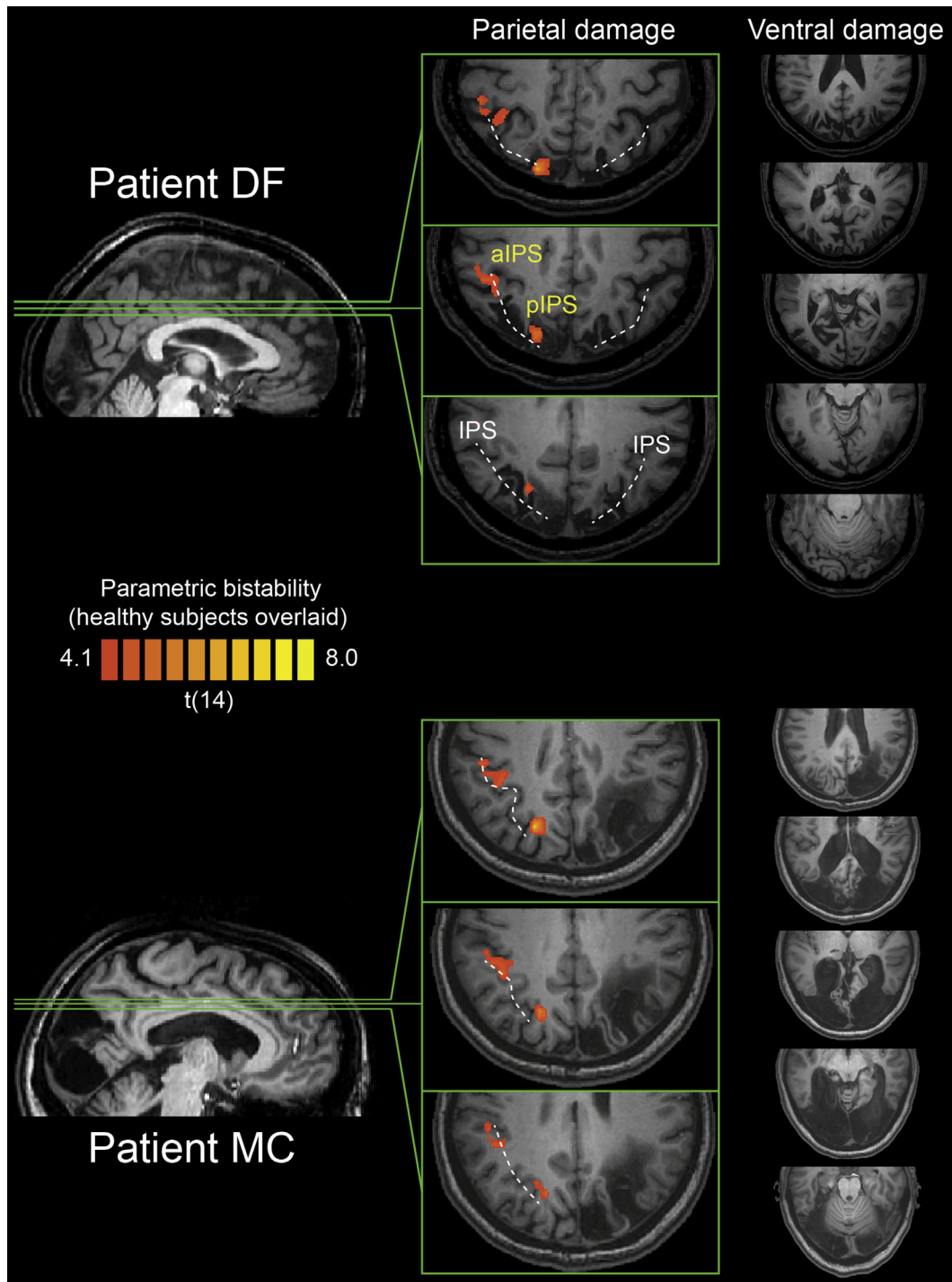
Fig. 8 — The parametric map of manual bistability activation (in healthy participants) was superimposed over the anatomical MRIs of DF and MC. Horizontal sections run dorsal (top) to ventral (bottom). At far left are mid-sagittal views of the three horizontal sections shown at center. Enlarged sections at center show lesions near the IPS (dotted line). Sections at far right show ventral lesions.

reaching depends upon the dorsal or ventral visual processing streams. Our patient experiment revealed that grasp postures selected with the contralesional hand are more likely to be awkward when the dorsal stream (i.e., pIPS or pSPL) is damaged. Moreover, the pIPS/pSPL lesions spatially overlapped with pIPS/pSPL parametric activation in neurologically intact participants performing the same task.

4.1.   Relation to previous patient studies

Our findings help to extend and reframe previous work on DF's unique pattern of deficits and preserved behaviors. Given the traditional picture of DF as predominantly, if not strictly, suffering from ventral stream pathology, Dijkerman et al. (2009) proposed that a perceptual analysis of object
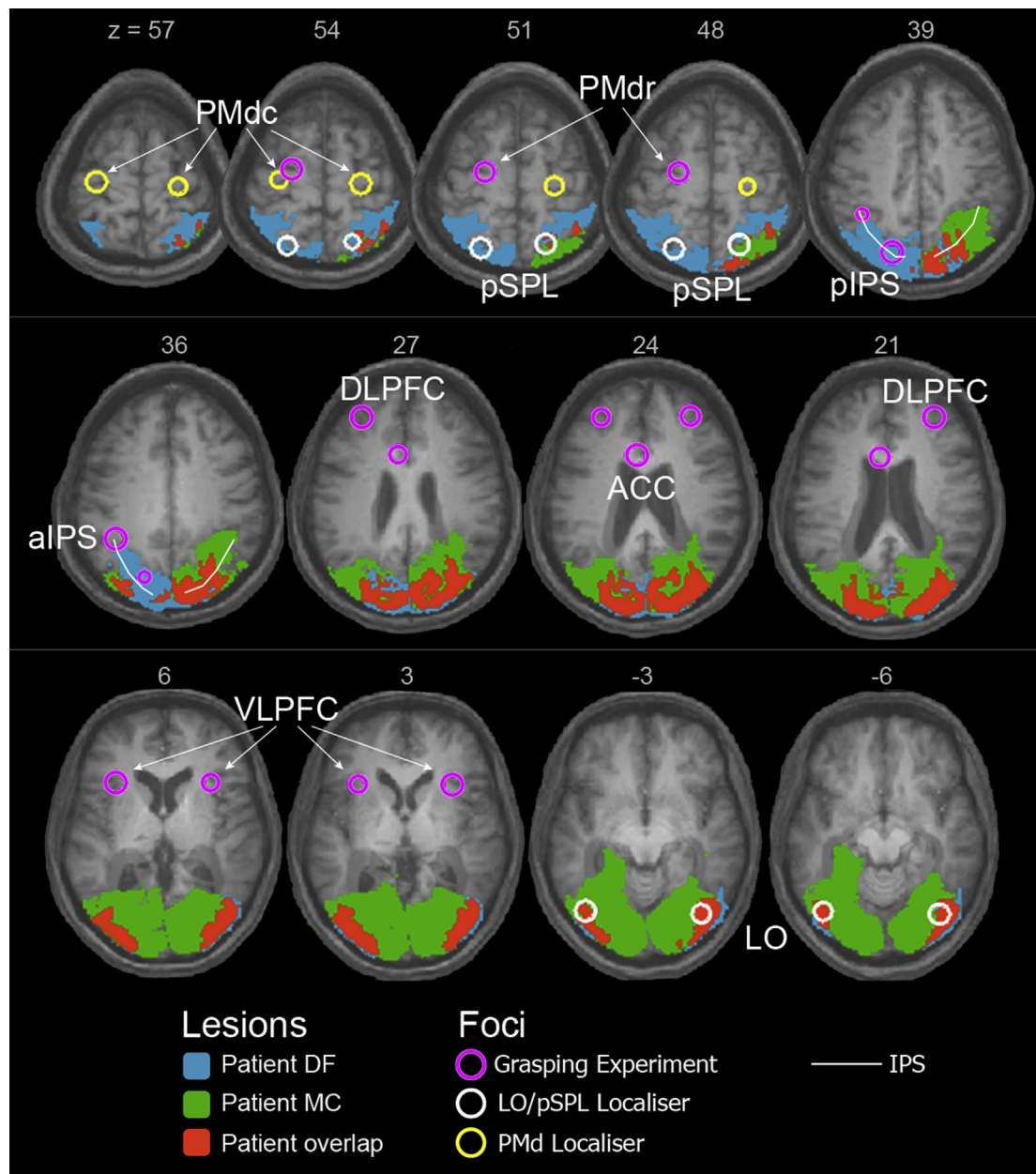
Fig. 9 — **Lesion maps (for MC and DF) and activation foci from the grasping and localizer fMRI experiments, superimposed over the average anatomical MRI in standardized space. Horizontal sections run dorsal (top left) to ventral (bottom right).**

orientation must be necessary for anticipating awkward movements. However, recent findings demonstrate that patient DF's brain damage is not confined to the ventral stream (Bridge et al., 2013); it includes bilateral thinning in posterior parietal cortex, extending to the posterior portions of the IPS and SPL (see Fig. 8), a region associated with the visual analysis of object orientation. Our results support the conclusion that DF's (and MC's) impaired posture selection is due to dorsal rather than ventral stream pathology.

We emphasize that DF's deficits in posture selection do not negate previous findings of her intact performance in a number of other reach-to-grasp tasks. Despite impaired perceptual identification of object shape or orientation (due to bilateral lesions in lateral occipital cortex), DF remains capable of optimally (Goodale et al., 1994) and accurately

scaling her fingers to the shape and orientation of objects during grasping (Goodale et al., 1991). Here, both MC and DF accurately scaled their hands to the bar in spite of pathological postural strategies. This demonstrates that MC and DF do not lack access to visual information about object orientation for the control of reach-to-grasp movements. Rather, there is a disruption either of the conversion of visual orientation into a prediction of the biomechanical cost, or of the decision process that regulates competition between movement alternatives. Our experiments yielded two important outcomes: (1) MC's healthy right-handed performance, in spite of bilateral LO lesions, demonstrates that intact LO cortex is not necessary for selecting postures on the basis of biomechanical cost, and (2) both patients selected extreme postures only if contralateral pIPS/pSPL was damaged. Taken together, these

findings highlight how the everyday behavior of selecting limb postures on the basis of biomechanical costs depends on the integrity of the dorsal stream.

One limitation of our approach is that, while the behavioral task required the same precision grip posture as past studies (Dijkerman et al., 2009; Stelmach et al., 1994), our fMRI task required a four-finger pinch grip. This difference in grip posture potentially complicates comparisons with other studies, and raises the possibility that non-overlapping brain regions are recruited for the different tasks. However, the primary difference between these tasks resides in the differential demands on fingertip precision. In both tasks, postural decisions were based primarily on wrist rotation. Indeed, we opted to use the pinch grip in the fMRI task because it encouraged wrist rotation and discouraged accommodations of the constrained MRI environment with a finger-based rotation of the thumb-finger axis (which we observed during piloting with the precision grip in the scanner). We also observed no systematic differences in posture selection between the two tasks. For these reasons, we believe the two tasks are comparable, and that the differences in fingertip precision are orthogonal to the goals of the present study.

We did not collect white-matter tractography from the two patients and a control population. Thus, we cannot rule out the possibility that the deficits observed in DF and MC were due to lesions on fibers connecting pIPS/pSPL to some other critical region that was still intact. To reiterate, however, we can rule out that this critical region is in LO, given that MC's right-hand performance was not impaired in spite of bilateral LO lesions. Even without access to tractography, our results warrant the interpretation that pIPS/pSPL play a non-redundant role in the network that mediates the selection of biomechanically viable postures.

4.2. Motor and decision variables in the fMRI experiment

For the fMRI analysis, we did not independently characterize biomechanical cost, but instead inferred costs from the postural preferences of individual participants. We make the assumption that some sort of biomechanical cost is driving posture preferences, but the precise identity of this cost was not a primary concern for this study. For our purposes, we operationally defined biomechanical cost as limb rotation, which we assumed was a straightforward function of wrist posture (i.e., thumb-left or -right) and stimulus orientation. Higher level cost terms such as end-point mobility (Cos et al., 2011) and end-state comfort (Rosenbaum & Jorgensen, 1992), both of which predictively bias the selection of global movement strategies (e.g., "Which movement should I perform?"), are presumably derived from a history of reinforcement learning with cost terms at the level of motor control (e.g., "How can I perform that movement?"). These latter costs may include muscle energy (Alexander, 1997; Guigon, Baraduc, & Desmurget, 2007), joint mobility (Soechting & Lacquaniti, 1981), and muscle tension (Dornay, Kawato, & Suzuki, 1996), among others. Most of these costs should be highly correlated with limb rotation in our task.

In our task, manual bistability occurred at stimulus orientations that required high levels of limb rotation (see Fig. 1B). Not surprisingly, increased limb rotation is associated with increased movement time (van Bergen, van Swieten, Williams, & Mon-Williams, 2007). Due to the approximately linear summation of the BOLD response over time, a more prolonged neural response will result in a higher magnitude BOLD response, even if the firing rate remains constant (Yarkoni, Barch, Gray, Conturo, & Braver, 2009). Thus, it is worth considering that our fMRI results may have been driven by parametric effects on movement time. However, a number of considerations make this unlikely. First, we would have expected limb rotation differences at a given orientation to result in robust, statistically significant differences in BOLD activation; we did not observe this (see Results, Section 3.4). Second, primary motor cortex, which is the cortical area most closely tied to the execution of voluntary movement, was not significantly activated in a parametric manner by our task (see Results, Section 3.2). Third, there is the issue of overlap between healthy parietal activation and the patient lesions; it is not clear why rather specific impairments in predicting postural comfort would result from lesions to a parietal area that is merely parametrically activated by motor execution.

A similar point can be made about RT. RT increases with the difficulty of a sensorimotor decision due to a decrease in the rate of evidence accumulation (Roitman & Shadlen, 2002). We have previously shown that RTs increase with bistability in the wrist posture selection task (Wood & Goodale, 2011), presumably due to a lack of strong sensory evidence in favor of one posture over another. We replicated this result in the control subjects for the behavioral experiment. We did not measure RT in the fMRI experiment, but it is likely that RT correlated positively with bistability here as well. The parametric design of our fMRI experiment should therefore be sensitive to prolonged processing precisely in those areas where postural decisions are computed. In other words, even if RT was correlated with bistability in the fMRI experiment, it functioned as a marker of competition or decision difficulty, rather than as a confounding variable.

4.3. Addressing the full range of activation in the fMRI experiment

We observed robust bilateral activation of pSPL and PMdc in the ROI analysis. Initially, this seems to be at odds with our patient results, which point to an elevated importance of contralateral processing during this task. However, the bilateral recruitment we observed could be indicative that ipsilateral activation contributes to—but is not absolutely necessary for—posture selection. Another possibility is that ipsilateral activation reflected covert decision processes for left-handed reaching. This is broadly consistent with previous work showing that application of transcranial magnetic stimulation (TMS) to pIPS shifted, by a few degrees, the preference between left- and right-handed reaches toward a target that varied in lateral position (Oliveira, Diedrichsen, Verstynen, Duque, & Ivry, 2010). While perturbing limb preference is not the same as inducing a deficit in posture selection, the underlying mechanisms could be similar; inter-hemispheric competition between limb preferences should be sensitive to the biomechanical costs of using a particular limb for a given target location. Indeed, we suggest that multistability due to biomechanical cost may be a motor

control phenomenon found in effector-specific regions throughout the dorsal stream. This would explain our observation of robust activation in the anterior intraparietal sulcus (aIPS), which is an area that combines visual and proprioceptive information to control digit placement during grasping movements (Culham et al., 2003; Makin, Holmes, & Zohary, 2007).

It should also be noted that there were spatial inconsistencies between the ROI and parametric activation foci, ranging between ~12 and 16 mm apart between experiments. Some degree of inconsistency is expected given that the task demands between the fMRI grasping and localizer experiments were different, which is an oft-cited weakness and criticism to the functional localization approach to fMRI (Friston, Rotshtein, Geng, Sterzer, & Henson, 2006). In our case, we had to rule out that the lack of an effect in LO using a whole-brain analysis could be due to a lack of sensitivity, which is inherently problematic for voxel-wise analysis due to the variability of sulcal anatomy in standardized Talairach space and the need to correct for multiple voxels in the whole brain (Saxe, Brett, & Kanwisher, 2006). Thus, by defining LO using functional localization, we verified that LO is likely not to have a role in determining wrist posture selection during our task. In addition, we further demonstrated that slightly different subdivisions of PMd and the SPL also have a role to play.

The initial motivation for the parametric design of our fMRI experiment was derived from the hypothesis that postural bistability occurs when cell populations have preferences for mutually exclusive movement strategies but are nonetheless simultaneously activated by a single stimulus (Cisek, 2007). The simultaneous activation of these two populations should, in theory, result in a stronger BOLD response (Durston et al., 2003). Our findings were consistent with this hypothesis. For example, variations of the parieto-frontal network that was activated by manual bistability in the present study (e.g., anterior cingulate cortex − ACC, VLPFC, DLPFC, PMd, aIPS, pIPS) have been observed in a number of other studies that manipulated response conflict (Fan et al., 2007; Liu, Banich, Jacobson, & Tanabe, 2004; Milham, Banich, & Barad, 2003; van Veen & Carter, 2005). The ACC is activated in situations of competition due to ambiguity (Bilenko, Grindrod, Myers, & Blumstein, 2009; Krain, Wilson, Arbuckle, Castellanos, & Milham, 2006) and response conflict (Botvinick, Cohen, & Carter, 2004; Botvinick, Nystrom, Fissell, Carter, & Cohen, 1999; Mansouri, Tanaka, & Buckley, 2009). Mechanisms in VLPFC appear to mediate the selection and retrieval of task-relevant knowledge over competing irrelevant knowledge (Badre, Poldrack, Paré-Blagoev, Insler, & Wagner, 2005). During ambiguous or competitive sensorimotor processing, DLPFC integrates sensory evidence (Domenech & Drew, 2010; Heekeren, Marrett, Bandettini, & Ungerleider, 2004), amplifies task-relevant information in sensorimotor areas (Egner & Hirsch, 2005), and modulates the avoidance of potentially risky or costly alternatives (Fecteau et al., 2007). Also, areas PMd and aIPS encode competing motor plans in parallel (Baumann, Fluet, & Scherberger, 2009; Chouinard & Goodale, 2009; Cisek & Kalaska, 2005).

Additional work has shown that PMd is critical in the selection of actions across a number of different response modalities (for review, see Chouinard, Leonard, & Paus, 2005; Chouinard & Paus, 2006, 2010), is frequently co-activated with areas in the SPL (Chouinard & Paus, 2006), and has strong connections with pIPS in monkeys (Matelli, Govoni, Galletti, Kutz, & Luppino, 1998) and humans (Chouinard, Van Der Werf, Leonard, & Paus, 2003; Tomassini et al., 2007). The results from the present study demonstrate that a PMd–pIPS circuit may be critical for the selection of biomechanically viable grasping postures.

4.4. Implications for LO and pIPS/pSPL

Our task measured wrist posture preferences as a function of visual object orientation (Kelso et al., 1994; Stelmach et al., 1994; Wood & Goodale, 2011). Sensitivity to orientation is found in both ventral and dorsal visual streams. In the ventral stream, a subregion of LO encodes object orientation (Silson et al., 2013). In the dorsal stream, a number of subdivisions in the SPL (including V6A, pIPS, and medial IPS) encode visual object orientation (Galletti, Fattori, Gamberini, & Kutz, 1999; Galletti, Fattori, Kutz, & Gamberini, 1999; Shikata et al., 2003; Valyear et al., 2006) and hand orientation during reaching (Fattori et al., 2009; Monaco et al., 2011). This shared sensitivity to object orientation allowed us to independently and simultaneously localize pSPL and LO by having participants passively view objects at different orientations. Between these two, only pSPL was also parametrically modulated by manual bistability.

Further, the awkward postures that characterized the impaired performance of DF and MC are reminiscent of the awkward grasp postures displayed by monkeys with lesions in area V6A (Battaglini et al., 2002), which is located in the pSPL and is near to pIPS both anatomically and functionally. This is in agreement with previous evidence that pIPS/pSPL plays an important role in combining visual, proprioceptive, and motor signals into a common reference frame (Beurze, de Lange, Toni, & Medendorp, 2007; McGuire & Sabes, 2011). The fact that pIPS/pSPL also appears to be critical to the proprioceptive guidance of the arm during reaching suggests a possible mechanism for incorporating knowledge of biomechanical constraints into the sensorimotor transformation of visual object orientation to appropriate hand and wrist orientation (Corradi-Dell'Acqua, Hesse, Rumiati, & Fink, 2008; Corradi-Dell'Acqua, Tomasino, & Fink, 2009; de Lange, Helmich, & Toni, 2006; Parkinson, Condon, & Jackson, 2010; Reichenbach, Thielscher, Peer, Bülthoff, & Bresciani, 2014; Rushworth, Johansen-Berg, & Young, 1998; Rushworth, Nixon, & Passingham, 1997; Sakata, Takaoka, Kawarasaki, & Shibutani, 1973). Neither of our experiments yielded evidence to support the hypothesis that any equivalent operation is performed by the ventral stream, suggesting that these fine-grained postural decisions can be carried out in the absence of a detailed perceptual analysis of object shape and orientation.

Competing financial interests

The authors declare no competing financial interests.

Acknowledgments

REFERENCES

Alexander, R. M. (1997). A minimum energy cost hypothesis for human arm trajectories. *Biological Cybernetics, 76*(2), 97—105.

Amiez, C., Kostopoulos, P., Champod, A.-S., & Petrides, M. (2006). Local morphology predicts functional organization of the dorsal premotor region in the human brain. *The Journal of Neuroscience: the Official Journal of the Society for Neuroscience, 26*(10), 2724—2731. http://doi.org/10.1523/JNEUROSCI.4739-05.2006.

Astafiev, S. V., Stanley, C. M., Shulman, G. L., & Corbetta, M. (2004). Extrastriate body area in human occipital cortex responds to the performance of motor actions. *Nature Neuroscience, 7*(5), 542—548. http://doi.org/10.1038/nn1241.

Badre, D., Poldrack, R. A., Paré-Blagoev, E. J., Insler, R. Z., & Wagner, A. D. (2005). Dissociable controlled retrieval and generalized selection mechanisms in ventrolateral prefrontal cortex. *Neuron, 47*(6), 907—918. http://doi.org/10.1016/j.neuron.2005.07.023.

Bardy, B. G., Oullier, O., Bootsma, R. J., & Stoffregen, T. A. (2002). Dynamics of human postural transitions. *Journal of Experimental Psychology: Human Perception and Performance, 28*(3), 499—514.

Battaglini, P. P., Muzur, A., Galletti, C., Skrap, M., Brovelli, A., & Fattori, P. (2002). Effects of lesions to area V6A in monkeys. *Experimental Brain Research Experimentelle Hirnforschung Expérimentation Cérébrale, 144*(3), 419—422. http://doi.org/10.1007/s00221-002-1099-4.

Baumann, M. A., Fluet, M.-C., & Scherberger, H. (2009). Context-specific grasp movement representation in the macaque anterior intraparietal area. *The Journal of Neuroscience: the Official Journal of the Society for Neuroscience, 29*(20), 6436—6448. http://doi.org/10.1523/JNEUROSCI.5479-08.2009.

van Bergen, E., van Swieten, L. M., Williams, J. H. G., & Mon-Williams, M. (2007). The effect of orientation on prehension movement time. *Experimental Brain Research Experimentelle Hirnforschung Expérimentation Cérébrale, 178*(2), 180—193. http://doi.org/10.1007/s00221-006-0722-1.

Beurze, S. M., de Lange, F. P., Toni, I., & Medendorp, W. P. (2007). Integration of target and effector information in the human brain during reach planning. *Journal of Neurophysiology, 97*(1), 188—199. http://doi.org/10.1152/jn.00456.2006.

Bilenko, N. Y., Grindrod, C. M., Myers, E. B., & Blumstein, S. E. (2009). Neural correlates of semantic competition during processing of ambiguous words. *Journal of Cognitive Neuroscience, 21*(5), 960—975. http://doi.org/10.1162/jocn.2009.21073.

Blake, R., & Logothetis, N. K. (2002). Visual competition. *Nature Reviews Neuroscience, 3*(1), 13—21. http://doi.org/10.1038/nrn701.

Bonda, E., Frey, S. H., & Petrides, M. (1996). Evidence for a dorso-medial parietal system involved in mental transformations of the body. *Journal of Neurophysiology, 76*(3), 2042—2048.

Bonda, E., Petrides, M., Frey, S. H., & Evans, A. (1995). Neural correlates of mental transformations of the body-in-space. *Proceedings of the National Academy of Sciences of the United States of America, 92*(24), 11180—11184.

Botvinick, M. M., Cohen, J. D., & Carter, C. S. (2004). Conflict monitoring and anterior cingulate cortex: an update. *Trends in Cognitive Sciences, 8*(12), 539—546.

Botvinick, M. M., Nystrom, L. E., Fissell, K., Carter, C. S., & Cohen, J. D. (1999). Conflict monitoring versus selection-for-action in anterior cingulate cortex. *Nature, 402*(6758), 179—181. http://doi.org/10.1038/46035.

Brainard, D. H. (1997). The Psychophysics Toolbox. *Spatial Vision, 10*(4), 433—436.

Bridge, H., Thomas, O. M., Minini, L., Cavina-Pratesi, C., Milner, A. D., & Parker, A. J. (2013). Structural and functional changes across the visual cortex of a patient with visual form agnosia. *The Journal of Neuroscience: the Official Journal of the Society for Neuroscience, 33*(31), 12779—12791. http://doi.org/10.1523/JNEUROSCI.4853-12.2013.

Buchanan, J. J., Kelso, J. A., & Fuchs, A. (1996). Coordination dynamics of trajectory formation. *Biological Cybernetics, 74*(1), 41—54.

Chouinard, P. A., & Goodale, M. A. (2009). FMRI adaptation during performance of learned arbitrary visuomotor conditional associations. *NeuroImage, 48*(4), 696—706. http://doi.org/10.1016/j.neuroimage.2009.07.020.

Chouinard, P. A., Leonard, G., & Paus, T. (2005). Role of the primary motor and dorsal premotor cortices in the anticipation of forces during object lifting. *The Journal of Neuroscience: the Official Journal of the Society for Neuroscience, 25*(9), 2277—2284. http://doi.org/10.1523/JNEUROSCI.4649-04.2005.

Chouinard, P. A., & Paus, T. (2006). The primary motor and premotor areas of the human cerebral cortex. *The Neuroscientist: a Review Journal Bringing Neurobiology, Neurology and Psychiatry, 12*(2), 143—152. http://doi.org/10.1177/1073858405284255.

Chouinard, P. A., & Paus, T. (2010). What have we learned from "perturbing" the human cortical motor system with transcranial magnetic stimulation? *Frontiers in Human Neuroscience, 4*, 173. http://doi.org/10.3389/fnhum.2010.00173.

Chouinard, P. A., Van Der Werf, Y. D., Leonard, G., & Paus, T. (2003). Modulating neural networks with transcranial magnetic stimulation applied over the dorsal premotor and primary motor cortices. *Journal of Neurophysiology, 90*(2), 1071—1083. http://doi.org/10.1152/jn.01105.2002.

Cisek, P. (2007). Cortical mechanisms of action selection: the affordance competition hypothesis. *Philosophical Transactions of the Royal Society of London. Series B, Biological Sciences, 362*(1485), 1585.

Cisek, P., & Kalaska, J. F. (2005). Neural correlates of reaching decisions in dorsal premotor cortex: specification of multiple direction choices and final selection of action. *Neuron, 45*(5), 801—814. http://doi.org/10.1016/j.neuron.2005.01.027.

Collins, D. L., Neelin, P., Peters, T. M., & Evans, A. C. (1994). Automatic 3D intersubject registration of MR volumetric data in standardized Talairach space. *Journal of Computer Assisted Tomography, 18*(2), 192—205.

Corradi-Dell'Acqua, C., Hesse, M. D., Rumiati, R. I., & Fink, G. R. (2008). Where is a nose with respect to a foot? The left posterior parietal cortex processes spatial relationships among body parts. *Cerebral Cortex (New York, NY: 1991), 18*(12), 2879—2890. http://doi.org/10.1093/cercor/bhn046.

Corradi-Dell'Acqua, C., Tomasino, B., & Fink, G. R. (2009). What is the position of an arm relative to the body? Neural correlates of body schema and body structural description. *The Journal of Neuroscience: the Official Journal of the Society for Neuroscience, 29*(13), 4162—4171. http://doi.org/10.1523/JNEUROSCI.4861-08.2009.

Cos, I., Bélanger, N., & Cisek, P. (2011). The influence of predicted arm biomechanics on decision making. *Journal of*

Neurophysiology, 105(6), 3022–3033. http://doi.org/10.1152/jn. 00975.2010.

Cos, I., Medleg, F., & Cisek, P. (2012). The modulatory influence of end-point controllability on decisions between actions. *Journal of Neurophysiology, 108*(6), 1764–1780. http://doi.org/10.1152/jn. 00081.2012.

Crajé, C., van der Kamp, J., & Steenbergen, B. (2008). The effect of the "rod-and-frame" illusion on grip planning in a sequential object manipulation task. *Experimental Brain Research Experimentelle Hirnforschung Expérimentation Cérébrale, 185*(1), 53–62. http://doi.org/10.1007/s00221-007-1130-x.

Crawford, J. R., Garthwaite, P. H., Howell, D. C., & Gray, C. D. (2004). Inferential methods for comparing a single case with a control sample: modified *t*-tests versus Mycroft et al.'s (2002) modified ANOVA. *Cognitive Neuropsychology, 21*(7), 750–755. http://doi.org/10.1080/02643290342000276.

Culham, J. C., Danckert, S. L., DeSouza, J. F. X., Gati, J. S., Menon, R. S., & Goodale, M. A. (2003). Visually guided grasping produces fMRI activation in dorsal but not ventral stream brain areas. *Experimental Brain Research Experimentelle Hirnforschung Expérimentation Cérébrale, 153*(2), 180–189. http://doi.org/10.1007/s00221-003-1591-5.

Dijkerman, H. C., Mcintosh, R. D., Schindler, I., Nijboer, T. C. W., & Milner, A. D. (2009). Choosing between alternative wrist postures: action planning needs perception. *Neuropsychologia, 47*(6), 1476–1482. http://doi.org/10.1016/j.neuropsychologia. 2008.12.002.

Domenech, P., & Drew, T. (2010). Decision threshold modulation in the human brain. *The Journal of Neuroscience: the Official Journal of the Society for Neuroscience, 30*(43), 14305–14317. http://doi.org/10.1523/JNEUROSCI.2371-10.2010.

Dornay, M., Kawato, A., & Suzuki, R. (1996). Minimum muscle-tension change trajectories predicted by using a 17-muscle model of the monkey's arm. *Journal of Motor Behavior, 28*(2), 83–100. http://doi.org/10.1080/00222895.1996.9941736.

Durston, S., Davidson, M. C., Thomas, K. M., Worden, M. S., Tottenham, N., Martinez, A., et al. (2003). Parametric manipulation of conflict and response competition using rapid mixed-trial event-related fMRI. *NeuroImage, 20*(4), 2135–2141. http://doi.org/10.1016/j.neuroimage.2003.08.004.

Dutton, G. N. (2003). Cognitive vision, its disorders and differential diagnosis in adults and children: knowing where and what things are. *Eye (London, England), 17*(3), 289–304. http://doi.org/10.1038/sj.eye.6700344.

Dyde, R. T., & Milner, A. D. (2002). Two illusions of perceived orientation: one fools all of the people some of the time; the other fools all of the people all of the time. *Experimental Brain Research Experimentelle Hirnforschung Expérimentation Cérébrale, 144*(4), 518–527. http://doi.org/10.1007/s00221-002-1065-1.

Egner, T., & Hirsch, J. (2005). Cognitive control mechanisms resolve conflict through cortical amplification of task-relevant information. *Nature Neuroscience, 8*(12), 1784–1790. http://doi.org/10.1038/nn1594.

Fan, J., Kolster, R., Ghajar, J., Suh, M., Knight, R., Sarkar, R., et al. (2007). Response anticipation and response conflict: an event-related potential and functional magnetic resonance imaging study. *The Journal of Neuroscience: the Official Journal of the Society for Neuroscience, 27*(9), 2272.

Fattori, P., Breveglieri, R., Marzocchi, N., Filippini, D., Bosco, A., & Galletti, C. (2009). Hand orientation during reach-to-grasp movements modulates neuronal activity in the medial posterior parietal area V6A. *The Journal of Neuroscience: the Official Journal of the Society for Neuroscience, 29*(6), 1928–1936. http://doi.org/10.1523/JNEUROSCI.4998-08.2009.

Fecteau, S., Pascual-Leone, A., Zald, D. H., Liguori, P., Théoret, H., Boggio, P. S., et al. (2007). Activation of prefrontal cortex by transcranial direct current stimulation reduces appetite for risk during ambiguous decision making. *The Journal of Neuroscience: the Official Journal of the Society for Neuroscience, 27*(23), 6212–6218. http://doi.org/10.1523/JNEUROSCI.0314-07. 2007.

Ferri, F., Frassinetti, F., Ardizzi, M., Costantini, M., & Gallese, V. (2012). A sensorimotor network for the bodily self. *Journal of Cognitive Neuroscience, 24*(7), 1584–1595. http://doi.org/10.1162/jocn_a_00230.

Friston, K. J., Rotshtein, P., Geng, J. J., Sterzer, P., & Henson, R. N. (2006). A critique of functional localisers. *NeuroImage, 30*(4), 1077–1087. http://doi.org/10.1016/j.neuroimage.2005.08.012.

Galletti, C., Fattori, P., Gamberini, M., & Kutz, D. F. (1999). The cortical visual area V6: brain location and visual topography. *The European Journal of Neuroscience, 11*(11), 3922–3936.

Galletti, C., Fattori, P., Kutz, D. F., & Gamberini, M. (1999). Brain location and visual topography of cortical area V6A in the macaque monkey. *The European Journal of Neuroscience, 11*(2), 575–582.

Glover, S., Dixon, P., Castiello, U., & Rushworth, M. (2005). Effects of an orientation illusion on motor performance and motor imagery. *Experimental Brain Research Experimentelle Hirnforschung Expérimentation Cérébrale, 166*(1), 17–22.

Goodale, M. A., Meenan, J. P., Bulthoff, H. H., Nicolle, D. A., Murphy, K. J., & Racicot, C. I. (1994). Separate neural pathways for the visual analysis of object shape in perception and prehension. *Current Biology: CB, 4*(7), 604–610.

Goodale, M. A., & Milner, A. D. (1992). Separate visual pathways for perception and action. *Trends in Neurosciences, 15*(1), 20–25.

Goodale, M. A., Milner, A. D., Jakobson, L. S., & Carey, D. P. (1991). A neurological dissociation between perceiving objects and grasping them. *Nature, 349*(6305), 154–156. http://doi.org/10. 1038/349154a0.

Goodale, M. A., Wolf, M. E., Whitwell, R. L., Brown, L. E., Cant, J. S., Chapman, C. S., et al. (2008). Preserved motion processing and visuomotor control in a patient with large bilateral lesions of occipitotemporal cortex. *Journal of Vision, 8*(6), 371. http://doi. org/10.1167/8.6.371.

Guigon, E., Baraduc, P., & Desmurget, M. (2007). Computational motor control: redundancy and invariance. *Journal of Neurophysiology, 97*(1), 331–347. http://doi.org/10.1152/jn. 00290.2006.

Heekeren, H. R., Marrett, S., Bandettini, P. A., & Ungerleider, L. G. (2004). A general mechanism for perceptual decision-making in the human brain. *Nature, 431*(7010), 859–862. http://doi.org/ 10.1038/nature02966.

Johnson, S. H., Rotte, M., Grafton, S. T., Hinrichs, H., Gazzaniga, M. S., & Heinze, H.-J. (2002). Selective activation of a parietofrontal circuit during implicitly imagined prehension. *NeuroImage, 17*(4), 1693–1704.

Kelso, J. A. S., Buchanan, J., & Murata, T. (1994). Multifunctionality and switching in the coordination dynamics of reaching and grasping. *Human Movement Science, 13*(1), 63–94.

Kent, S. W., Wilson, A. D., Plumb, M. S., Williams, J. H. G., & Mon-Williams, M. (2009). Immediate movement history influences reach-to-grasp action selection in children and adults. *Journal of Motor Behavior, 41*(1), 10–15.

Krain, A. L., Wilson, A. M., Arbuckle, R., Castellanos, F. X., & Milham, M. P. (2006). Distinct neural mechanisms of risk and ambiguity: a meta-analysis of decision-making. *NeuroImage, 32*(1), 477–484. http://doi.org/10.1016/j.neuroimage.2006.02.047.

de Lange, F. P., Helmich, R. C., & Toni, I. (2006). Posture influences motor imagery: an fMRI study. *NeuroImage, 33*(2), 609–617. http://doi.org/10.1016/j.neuroimage.2006.07.017.

Leopold, D., & Logothetis, N. (1999). Multistable phenomena: changing views in perception. *Trends in Cognitive Sciences, 3*(7), 254–264.

Liu, X., Banich, M. T., Jacobson, B. L., & Tanabe, J. L. (2004). Common and distinct neural substrates of attentional control in an integrated Simon and spatial Stroop task as assessed by

event-related fMRI. *NeuroImage, 22*(3), 1097–1106. http://doi.org/10.1016/j.neuroimage.2004.02.033.

Makin, T. R., Holmes, N. P., & Zohary, E. (2007). Is that near my hand? Multisensory representation of peripersonal space in human intraparietal sulcus. *The Journal of Neuroscience: the Official Journal of the Society for Neuroscience, 27*(4), 731–740. http://doi.org/10.1523/JNEUROSCI.3653-06.2007.

Mansouri, F. A., Tanaka, K., & Buckley, M. J. (2009). Conflict-induced behavioural adjustment: a clue to the executive functions of the prefrontal cortex. *Nature Reviews Neuroscience, 10*(2), 141–152. http://doi.org/10.1038/nrn2538.

Matelli, M., Govoni, P., Galletti, C., Kutz, D., & Luppino, G. (1998). Superior area 6 afferents from the superior parietal lobule in the macaque monkey. *The Journal of Comparative Neurology, 402*(3), 327–352.

McGuire, L. M. M., & Sabes, P. N. (2011). Heterogeneous representations in the superior parietal lobule are common across reaches to visual and proprioceptive targets. *The Journal of Neuroscience: the Official Journal of the Society for Neuroscience, 31*(18), 6661–6673. http://doi.org/10.1523/JNEUROSCI.2921-10.2011.

Milham, M. P., Banich, M. T., & Barad, V. (2003). Competition for priority in processing increases prefrontal cortex's involvement in top-down control: an event-related fMRI study of the Stroop task. *Brain Research Cognitive Brain Research, 17*(2), 212–222.

Monaco, S., Cavina-Pratesi, C., Sedda, A., Fattori, P., Galletti, C., & Culham, J. C. (2011). Functional magnetic resonance adaptation reveals the involvement of the dorsomedial stream in hand orientation for grasping. *Journal of Neurophysiology, 106*(5), 2248–2263. http://doi.org/10.1152/jn.01069.2010.

Oldfield, R. C. (1971). The assessment and analysis of handedness: the Edinburgh inventory. *Neuropsychologia, 9*(1), 97–113.

Oliveira, F. T. P., Diedrichsen, J., Verstynen, T., Duque, J., & Ivry, R. B. (2010). Transcranial magnetic stimulation of posterior parietal cortex affects decisions of hand choice. *Proceedings of the National Academy of Sciences of the United States of America, 107*(41), 17751–17756. http://doi.org/10.1073/pnas.1006223107.

Parkinson, A., Condon, L., & Jackson, S. R. (2010). Parietal cortex coding of limb posture: in search of the body-schema. *Neuropsychologia, 48*(11), 3228–3234. http://doi.org/10.1016/j.neuropsychologia.2010.06.039.

Picard, N., & Strick, P. L. (2001). Imaging the premotor areas. *Current Opinion in Neurobiology, 11*(6), 663–672.

Reichenbach, A., Thielscher, A., Peer, A., Bülthoff, H. H., & Bresciani, J.-P. (2014). A key region in the human parietal cortex for processing proprioceptive hand feedback during reaching movements. *NeuroImage, 84*(C), 615–625. http://doi.org/10.1016/j.neuroimage.2013.09.024.

Roitman, J. D., & Shadlen, M. N. (2002). Response of neurons in the lateral intraparietal area during a combined visual discrimination reaction time task. *The Journal of Neuroscience: the Official Journal of the Society for Neuroscience, 22*(21), 9475–9489.

Rosenbaum, D. A., & Jorgensen, M. J. (1992). Planning macroscopic aspects of manual control. *Human Movement Science, 11*, 61–69.

Rosenbaum, D. A., Marchak, F., Barnes, H. J., Vaughan, J., Slotta, J. D., & Jorgensen, M. J. (1990). Constraints for action selection: overhand versus underhand grips. In *Attention and Performance XIII*.

Rushworth, M. F., Johansen-Berg, H., & Young, S. A. (1998). Parietal cortex and spatial–postural transformation during arm movements. *Journal of Neurophysiology, 79*(1), 478–482.

Rushworth, M. F. S., Nixon, P. D., & Passingham, R. E. (1997). Parietal cortex and movement: I. Movement selection and reaching. *Experimental Brain Research Experimentelle Hirnforschung Expérimentation Cérébrale, 117*(2), 292–310. http://doi.org/10.1007/s002210050224.

Sabes, P. N., & Jordan, M. I. (1997). Obstacle avoidance and a perturbation sensitivity model for motor planning. *The Journal of Neuroscience: the Official Journal of the Society for Neuroscience, 17*(18), 7119–7128.

Sakata, H., Takaoka, Y., Kawarasaki, A., & Shibutani, H. (1973). Somatosensory properties of neurons in the superior parietal cortex (area 5) of the rhesus monkey. *Brain Research, 64*, 85–102.

Saxe, R., Brett, M., & Kanwisher, N. (2006). Divide and conquer: a defense of functional localizers. *NeuroImage, 30*(4), 1088–1096. http://doi.org/10.1016/j.neuroimage.2005.12.062.

Shikata, E., Hamzei, F., Glauche, V., Koch, M., Weiller, C., Binkofski, F., et al. (2003). Functional properties and interaction of the anterior and posterior intraparietal areas in humans. *The European Journal of Neuroscience, 17*(5), 1105–1110. http://doi.org/10.1046/j.1460-9568.2003.02540.x.

Silson, E. H., McKeefry, D. J., Rodgers, J., Gouws, A. D., Hymers, M., & Morland, A. B. (2013). Specialized and independent processing of orientation and shape in visual field maps LO1 and LO2. *Nature Neuroscience, 1*–4. http://doi.org/10.1038/nn.3327.

Soechting, J. F., & Lacquaniti, F. (1981). Invariant characteristics of a pointing movement in man. *The Journal of Neuroscience: the Official Journal of the Society for Neuroscience, 1*(7), 710–720.

Stelmach, G. E., Castiello, U., & Jeannerod, M. (1994). Orienting the finger opposition space during prehension movements. *Journal of Motor Behavior, 26*(2), 178–186.

Sterzer, P., Kleinschmidt, A., & Rees, G. (2009). The neural bases of multistable perception. *Trends in Cognitive Sciences, 13*(7), 310–318. http://doi.org/10.1016/j.tics.2009.04.006.

Tomassini, V., Jbabdi, S., Klein, J. C., Behrens, T. E. J., Pozzilli, C., Matthews, P. M., et al. (2007). Diffusion-weighted imaging tractography-based parcellation of the human lateral premotor cortex identifies dorsal and ventral subregions with anatomical and functional specializations. *The Journal of Neuroscience: the Official Journal of the Society for Neuroscience, 27*(38), 10259–10269. http://doi.org/10.1523/JNEUROSCI.2144-07.2007.

Urgesi, C., Calvo-Merino, B., Haggard, P., & Aglioti, S. M. (2007). Transcranial magnetic stimulation reveals two cortical pathways for visual body processing. *The Journal of Neuroscience: the Official Journal of the Society for Neuroscience, 27*(30), 8023–8030. http://doi.org/10.1523/JNEUROSCI.0789-07.2007.

Urgesi, C., Candidi, M., Ionta, S., & Aglioti, S. M. (2007). Representation of body identity and body actions in extrastriate body area and ventral premotor cortex. *Nature Neuroscience, 10*(1), 30–31. http://doi.org/10.1038/nn1815.

Valyear, K. F., Culham, J. C., Sharif, N., Westwood, D., & Goodale, M. A. (2006). A double dissociation between sensitivity to changes in object identity and object orientation in the ventral and dorsal visual streams: a human fMRI study. *Neuropsychologia, 44*(2), 218–228. http://doi.org/10.1016/j.neuropsychologia.2005.05.004.

van Veen, V., & Carter, C. S. (2005). Separating semantic conflict and response conflict in the Stroop task: a functional MRI study. *NeuroImage, 27*(3), 497–504. http://doi.org/10.1016/j.neuroimage.2005.04.042.

Wolf, M. E., Whitwell, R. L., Brown, L. E., Cant, J. S., Chapman, C., Witt, J. K., et al. (2008). Preserved visual abilities following large bilateral lesions of the occipitotemporal cortex. *Journal of Vision, 8*(6), 624. http://doi.org/10.1167/8.6.624.

Wolpert, D. M., Goodbody, S. J., & Husain, M. (1998). Maintaining internal representations: the role of the human superior parietal lobe. *Nature Neuroscience, 1*(6), 529–533. http://doi.org/10.1038/2245.

Wood, D. K., & Goodale, M. A. (2011). Selection of wrist posture in conditions of motor ambiguity. *Experimental Brain Research Experimentelle Hirnforschung Expérimentation Cérébrale, 208*(4), 607–620. http://doi.org/10.1007/s00221-010-2509-7.

Worsley, K. J., Evans, A. C., Marrett, S., & Neelin, P. (1992). A three-dimensional statistical analysis for CBF activation studies in human brain. *Journal of Cerebral Blood Flow and Metabolism: Official Journal of the International Society of Cerebral Blood Flow and Metabolism, 12*(6), 900−918. http://doi.org/10.1038/jcbfm.1992.127.

Yarkoni, T., Barch, D. M., Gray, J. R., Conturo, T. E., & Braver, T. S. (2009). BOLD correlates of trial-by-trial reaction time variability in gray and white matter: a multi-study fMRI analysis. *PloS One, 4*(1), e4257. http://doi.org/10.1371/journal.pone.0004257.t002.

Zander, S. L., Weiss, D. J., & Judge, P. G. (2013). The interface between morphology and action planning: a comparison of two species of New World monkeys. *Animal Behaviour, 86,* 1251−1258.

Zimmermann, M., Meulenbroek, R. G. J., & de Lange, F. P. (2011). Motor planning is facilitated by adopting an action's goal posture: an fMRI study. *Cerebral Cortex (New York, NY: 1991), 22*(1), 122−131. http://doi.org/10.1093/cercor/bhr098.